Journal of Materials Chemistry A

ROYAL SOCIETY OF CHEMISTRY

PAPER

View Article Online
View Journal | View Issue

Open Access Article. Published on 27 September 2024. Downloaded on 4/2/2026 8:34:18 PM. This article is licensed under a Creative Commons Attribution-NonCommercial 3.0 Unported Licence.

Check for updates

Cite this: J. Mater. Chem. A, 2024, 12, 29138

Kinetic H_2S/CO_2 selectivity in an exceptionally sterically hindered amine membrane†

Shraavya Rao,[a] Xuepeng Deng,[a] Changlong Zou,[a] Babul Prasad,[ab] Yang Han,[a] Li-Chiang Lin[ac] and W.S. Winston Ho[*ad]

Received 18th July 2024
Accepted 26th September 2024

DOI: 10.1039/d4ta04997g

rsc.li/materials-a

Facilitated transport membranes (FTMs) show great promise for H_2S/CO_2 separation, an industrially important yet challenging process. Herein, we report FTMs with excellent H_2S/CO_2 separation performance and investigate how contradictory thermodynamic and kinetic reaction preferences affect FTM selectivity. For membranes based on an extremely sterically hindered di-*tert*-butylamine carrier, CO_2 transport occurs exclusively *via* a slow bicarbonate pathway. Reducing the membrane thickness shifts the reaction preference from the thermodynamically favored bicarbonate pathway to the kinetically favored amine-H_2S reaction, leading to a 10-fold improvement in H_2S/CO_2 selectivity. This unusual trend of increasing selectivity with decreasing thickness, the opposite of typical FTMs, enables simultaneous improvements in membrane permeance and selectivity. This translates to an exceptional H_2S/CO_2 permselectivity of 20, and an overall separation performance surpassing the H_2S/CO_2 upper bounds.

Introduction

H_2S and CO_2, both acidic gases, are common co-contaminants in fuel gases such as syngas and natural gas.[1–3] H_2S, a highly toxic gas, is lethal to humans at levels as low as 1000 ppm.[4,5] CO_2, while non-toxic, can cause corrosion damage to pipelines and equipment.[6,7] To minimize safety hazards, both CO_2 and H_2S must be removed from the fuels before further processing. This removal process produces a concentrated acid gas stream containing 80–90% CO_2 and 1–10% H_2S.[8,9] The H_2S must then be recovered and used for the production of elemental sulfur, an essential commodity in the agrochemicals industry.[10] Therefore, there is a need for developing low-cost technologies that can selectively separate H_2S from such CO_2-rich gases.[3,11–15]

The state-of-the-art technology for H_2S/CO_2 separation is absorption using sterically hindered amines.[16–22] However, absorption is often energy- and capital-intensive.[23] Moreover, treating highly acidic feeds can exacerbate corrosion, necessitating frequent maintenance and the use of expensive, corrosion-resistant materials.[23]

An alternative that avoids such drawbacks is the use of small-molecule amines as 'carriers' within a polymeric membrane. Such membranes, known as facilitated transport membranes (FTMs), avoid the need for solvent regeneration and offer advantages such as energy-efficiency and low susceptibility to corrosion.[24] Known for their superior separation performance, FTMs have attracted significant attention for CO_2 capture, and several researchers have investigated the use of FTMs for CO_2/inert gas separations.[25–32]

To date, very few papers examine selectivity between two reactive gases in FTMs, such as the case of H_2S/CO_2 separation.[33–37] These studies report H_2S/CO_2 selectivities of 3–5, which are similar to those of conventional polymeric membranes and insufficient for practical applications.[38–40] The poor selectivity stems from the competition between H_2S and CO_2 facilitation in typical amine FTMs.[34] In general, the equilibrium constants for the amine-CO_2 reactions (Fig. 1(a) and (b)) are much higher than that of the amine-H_2S reaction (Fig. 1(c)).[34] Most amine FTMs offer equilibrium-based separation, wherein the H_2S/CO_2 selectivity is compromised by competitive CO_2 facilitation.[34]

The key to improving the H_2S/CO_2 selectivity lies in the kinetic aspects of the competing reactions. The hydrosulfide and carbamate formation reactions are fast reactions—in fact, the amine-H_2S reaction is essentially instantaneous.[47] The bicarbonate formation reaction is known to be significantly slower, in part due to the lower probability of a termolecular collision.[20,42,43,45] Estimates suggest that bicarbonate formation

[a]William G. Lowrie Department of Chemical and Biomolecular Engineering, The Ohio State University, 151 West Woodruff Avenue, Columbus, OH 43210-1350, USA. E-mail: ho.192@osu.edu

[b]Polymer Science and Engineering Division, CSIR-National Chemical Laboratory, Dr Homi Bhabha Road, Pashan, Pune 411008, India

[c]Department of Chemical Engineering, National Taiwan University, Taipei 10617, Taiwan

[d]Department of Materials Science and Engineering, The Ohio State University, 2041 College Road, Columbus, OH 43210-1178, USA

† Electronic supplementary information (ESI) available. See DOI: https://doi.org/10.1039/d4ta04997g

This journal is © The Royal Society of Chemistry 2024

Open Access Article. Published on 27 September 2024. Downloaded on 4/2/2026 8:34:18 PM.
This article is licensed under a Creative Commons Attribution-NonCommercial 3.0 Unported Licence.

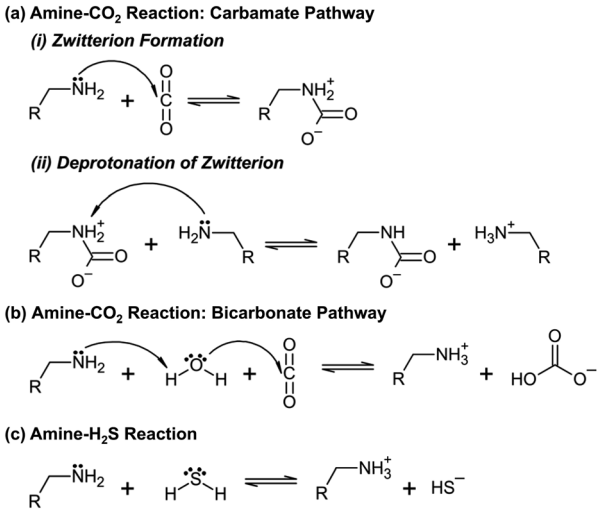

Fig. 1 Mechanisms for the amine-CO_2 and the amine-H_2S reactions.[41–46] R refers to an alkyl group or hydrogen. (a) The carbamate pathway of the amine-CO_2 reaction. In step (i), the lone pair of the N atom attacks CO_2 to form a zwitterionic intermediate. In step (ii), the zwitterion is deprotonated by another amine molecule to form a carbamate anion. Nucleophilic amines usually react *via* this pathway.[41,46] (b) The bicarbonate pathway of the amine-CO_2 reaction. A bicarbonate anion is formed by the amine-assisted hydration of CO_2. Sterically hindered amines, which cannot form stable carbamates, react through this pathway.[41,46] (c) The amine-H_2S reaction. H_2S loses a proton to the amine and forms hydrosulfide.[47] The reaction is independent of amine structure.

occurs on time scales of 0.01–1 second, while the carbamate and hydrosulfide reactions are approximately 10^3 and 10^5 times faster, respectively.[20,47,48] These distinct kinetic characteristics can be leveraged to devise a two-pronged approach for improving the H_2S/CO_2 permselectivity in FTMs. Firstly, CO_2 transport through the fast carbamate pathway must be suppressed. This can be achieved through the use of severely hindered amine carriers, which cannot form carbamates. Next, CO_2 transport as bicarbonate must be minimized. This requires FTMs with diffusion times lower than the time scale of the slow bicarbonate formation reaction. Such an FTM is expected to offer a kinetic selectivity for H_2S over CO_2.

To illustrate this, we compare two different carriers: potassium glycinate (Gly), a primary amine, and potassium *N*-hydroxy-*tert*-butyl aminoisobutyrate (TB-AIBA), an extremely hindered amine. Using density functional theory (DFT), ^{13}C nuclear magnetic resonance (NMR) and *in situ* Fourier transform infrared (FTIR) spectroscopy, we demonstrate that the TB-AIBA-based FTM, which transports CO_2 as bicarbonate, offers kinetically-controlled separation and exceptional H_2S/CO_2 selectivity. No such selectivity was observed for the carbamate-forming Gly-based FTM, wherein the separation was equilibrium-controlled.

Results and discussion

The synthesis of the carriers and membranes is described in brief here for convenience. A detailed description of the experimental procedures and the computational techniques used for the DFT simulations can be found in the ESI.† Gly is commercially available and was used as purchased. TB-AIBA was synthesized *via* the Bargellini reaction as per a literature method.[49,50] The carriers were incorporated into crosslinked poly(vinyl alcohol) (PVA). A crosslinking degree of 100% was selected in order to ensure that the coating solution had a good viscosity, allowing for the fabrication of thin-film composite membranes. Membranes were fabricated by coating onto a nanoporous polysulfone support layer, which provides mechanical strength. Extensive characterization using FTIR, X-ray photoelectron spectroscopy (XPS), and scanning electron microscopy (SEM), presented in Fig. 2, were used to confirm the successful synthesis of thin-film composite membranes.

Fig. 2(a) presents the FTIR spectra of crosslinked PVA and the PVA/carrier blends. As seen in the figure, the blends show a broad peak in the 3300 cm^{-1} region, which is absent in the pure PVA spectrum. The peak can be attributed to the NH stretching vibrations of the amino acids, with the broad bands indicating the presence of hydrogen bonding interactions between the amine group and the polymer matrix.[51] Fig. 2(b) depicts the XPS spectra of crosslinked PVA and the blend membranes. Peaks corresponding to the amine nitrogen and the potassium cation are clearly visible in the spectra of the blend membranes, indicating that the amino acid salts have been successfully incorporated into the membrane. Lastly, the cross-sectional SEM (Fig. 2(c)) shows a clearly distinguishable selective layer resting over the polysulfone support.

Gly, a popular carrier for CO_2-selective FTMs, is a nucleophilic amine.[52–56] Accordingly, Gly is expected to react primarily *via* nucleophilic attack to form carbamate (Fig. 3(a)), with minor, if at all any, bicarbonate formation.

Moreover, at reaction equilibrium, carbamate formation is expected to be preferred over hydrosulfide formation (Fig. 3(b)).[33,34] This is supported by DFT simulations. The thermodynamic product stabilities (ΔE, calculated as $E_{products} - E_{reactants}$), presented in Fig. 3(c), suggest a mild preference for carbamate ($\Delta E = -8.5$ kcal mol^{-1}) over hydrosulfide formation ($\Delta E = -7.1$ kcal mol^{-1}). Evidently, the reaction equilibrium favors CO_2 over H_2S. While the carbamate and bicarbonate products have similar stabilities, the activation energy barriers (E_a), presented in Fig. 3(d), suggest that bicarbonate formation is kinetically unfavorable ($E_a = 5.2$ kcal mol^{-1} for carbamate *vs.* $E_a = 12.4$ kcal mol^{-1} for bicarbonate). This is further supported by *in situ* FTIR (Fig. 3(e)) and ^{13}C NMR spectroscopy (Fig. 3(f)), which show that Gly forms predominantly carbamate, with bicarbonate being a minor product (see Table S1† for IR peak assignments).[55,57–63] The barrier for hydrosulfide formation is much lower ($E_a = 1.5$ kcal mol^{-1}) than those for the CO_2 reaction pathways, indicating that Gly shows a kinetic preference for H_2S. However, as we will show ahead, the relatively small difference in the activation barriers is insufficient to achieve kinetically-controlled separation within the Gly-based FTM.

Unlike Gly, TB-AIBA is an exceptionally sterically hindered amine and an extremely poor nucleophile (see Section S3† for comparison with other amines). Consequently, carbamate formation is highly unfavorable, and TB-AIBA is expected to

Open Access Article. Published on 27 September 2024. Downloaded on 4/2/2026 8:34:18 PM. This article is licensed under a Creative Commons Attribution-NonCommercial 3.0 Unported Licence.

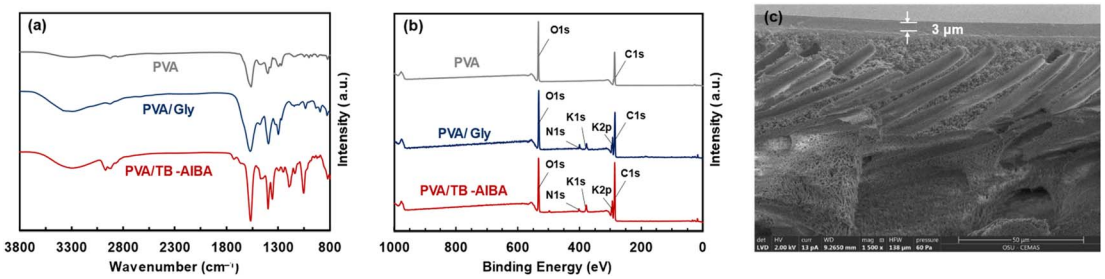

Fig. 2 Characterization of crosslinked PVA and blends incorporating Gly and TB-AIBA. (a) FTIR spectra of freestanding crosslinked PVA, PVA/Gly film and PVA/TB-AIBA film. (b) XPS spectra of crosslinked PVA, PVA/Gly film and PVA/TB-AIBA film. (c) Cross-sectional SEM of thin-film composite membrane containing TB-AIBA.

react with CO_2 exclusively through bicarbonate formation (Fig. 4(a)). The severe hindrance also negatively affects the rate of the bicarbonate pathway, further increasing the kinetic preference for hydrosulfide formation (Fig. 4(b)).[45] It should be mentioned that the hydroxyl moiety was deliberately incorporated into the carrier structure in order to mitigate issues of solubility and incompatibility arising from the bulky alkyl substituents.[15] Note that Gly and TB-AIBA exhibit similar water uptake levels.[15] Accordingly, reactive transport within the two FTMs is unlikely to be affected by differences in water uptake.

The thermodynamic product stabilities for the TB-AIBA-acid gas reactions (Fig. 4(c)) indicate that the reaction equilibrium favors bicarbonate over hydrosulfide ($\Delta E = -9$ kcal mol^{-1} for hydrosulfide *vs.* $\Delta E = -12$ kcal mol^{-1} for bicarbonate). Conversely, the kinetic barriers (Fig. 4(d)) indicate a strong kinetic preference for hydrosulfide formation over bicarbonate formation ($E_a = 2.3$ kcal mol^{-1} for hydrosulfide *vs.* $E_a = 13.1$ kcal mol^{-1} for bicarbonate). Note that the carbamate product is unstable ($\Delta E = 3$ kcal mol^{-1}) and will not form. This is again supported by the *in situ* FTIR (Fig. 4(e)) and ^{13}C NMR (Fig. 4(f)), which show bicarbonate formation but no indication of carbamate (see Table S2† for IR peak assignments).[55,59,61]

In short, both Gly and TB-AIBA show a thermodynamic preference for CO_2, and a kinetic preference for H_2S. Under conditions of equilibrium-controlled separation (*i.e.*, FTM systems with a Damköhler number Da $\gg$ 1 (ref. 64)), both FTMs will suffer from competitive CO_2 facilitation, leading to low selectivity. Amplifying the kinetic aspects of the competing reactions by minimizing the diffusion time is crucial to improving the H_2S/CO_2 selectivity. This is illustrated in Fig. 5(a), which presents the effect of FTM thickness on the H_2S/CO_2 selectivity. For the TB-AIBA FTM, which reacts with CO_2 through the slow bicarbonate pathway, the H_2S/CO_2 selectivity increases 10-fold from 2 to 20 as the membrane thickness decreases from 30 to 3 μm.

Decreasing the FTM thickness reduces the reaction time for the competing amine-H_2S and amine-CO_2 reactions, thus enhancing the selectivity for the "faster", kinetically favored product, *i.e.*, hydrosulfide. The effect of thickness can also be illustrated using the facilitated transport model developed by Dindi *et al.*[34] (see Section S3†). Accordingly, the 3 μm-thick TB-AIBA FTM displays a high H_2S/CO_2 selectivity of *ca.* 20. This is a remarkable improvement over conventional polymeric membranes, which can only offer selectivities of *ca.* 3–8.[38–40,65,66] An additional advantage of reducing the membrane thickness is the enhancement in H_2S permeance (see Table S3†).

Fig. 5(b) clearly shows that the kinetics-derived separation performances of the thinner TB-AIBA FTMs surpass the H_2S/CO_2 upper bounds and outperform literature data. This is in contrast to the Gly-based FTM, where the selectivity does not vary appreciably with thickness. Instead, the selectivity remains essentially constant at *ca.* 4, which indicates that the faster carbamate and hydrosulfide reactions are already close to equilibrium. Hence, varying the thickness does not affect the product distribution and thereby the H_2S/CO_2 selectivity.

It should be noted that humidity could have a strong impact on membrane performance. The effect of humidity on the H_2S/CO_2 separation properties will be further explored in a future publication. However, the gas mixture encountered in a practical application is typically saturated with water vapor at a given temperature. The future work will also involve long-term stability testing of the membrane, as the current setup only permits handling of toxic H_2S for short durations (*ca.* 8 h). However, good membrane stability can be expected based on the findings from our previous work, which utilized similar membrane components.[71] The membrane materials showed stable performance over a period of 264 h.

Having established that bicarbonate formation has been minimized in the 3 μm TB-AIBA FTM, we then examined the carrier saturation behavior in order to quantify the extent of H_2S and CO_2 facilitation (Fig. 6). Carrier saturation refers to the characteristic decrease in the permeance of the acid gas with increasing acid gas partial pressure, analogous to the sorption isotherms of amine adsorbents. As the partial pressure rises, an increasing number of carriers are consumed by the reaction. The number of free carriers decreases, causing a drop in the permeance. As with sorption isotherms, the carrier saturation curve provides valuable insights into the carrier-acid gas reaction mechanisms.

For the Gly-based FTM, the H_2S permeance does not vary substantially with feed composition. The H_2S permeance decreases only slightly, from 217 to 145 GPU, with increasing feed H_2S concentration. Correspondingly, the CO_2 permeance (see Table S3†) also decreases slightly, from *ca.* 60 to 40 GPU.

 This journal is © The Royal Society of Chemistry 2024

Open Access Article. Published on 27 September 2024. Downloaded on 4/2/2026 8:34:18 PM.
This article is licensed under a Creative Commons Attribution-NonCommercial 3.0 Unported Licence.

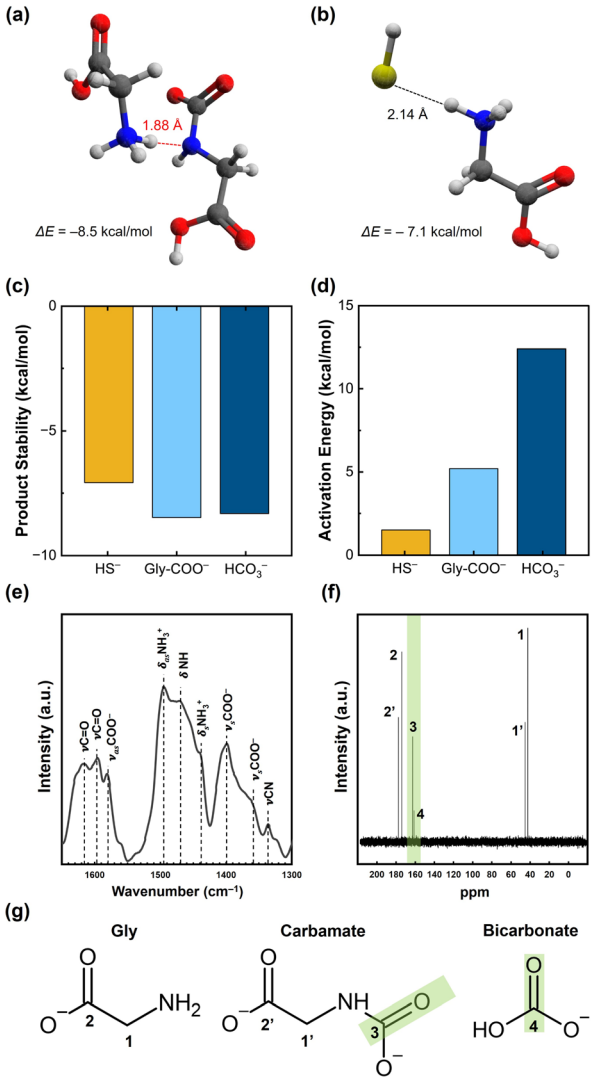

Fig. 3 Molecular configurations of (a) carbamate reaction products and (b) hydrosulfide reaction products for carrier Gly. Color code: carbon (grey), nitrogen (blue), oxygen (red), and hydrogen (white). Red dashed lines represent a hydrogen bond; black dashed lines represent the main atomic distance. DFT-computed (c) product stabilities, and (d) activation energy barriers for the reactions of Gly with H_2S and CO_2. (e) FTIR spectrum obtained upon *in situ* exposure of PVA/Gly FTM to 20% CO_2 in N_2 at 110 °C. (f) ^{13}C NMR spectrum obtained upon exposing a 0.5 M Gly solution to CO_2 at ambient temperature. The CO_2 loading was controlled to 0.2 M. (g) Chemical structures of Gly, the glycinate carbamate anion, and the bicarbonate anion. The numbering of the carbon atoms corresponds to the peak labels in subfigure (f).

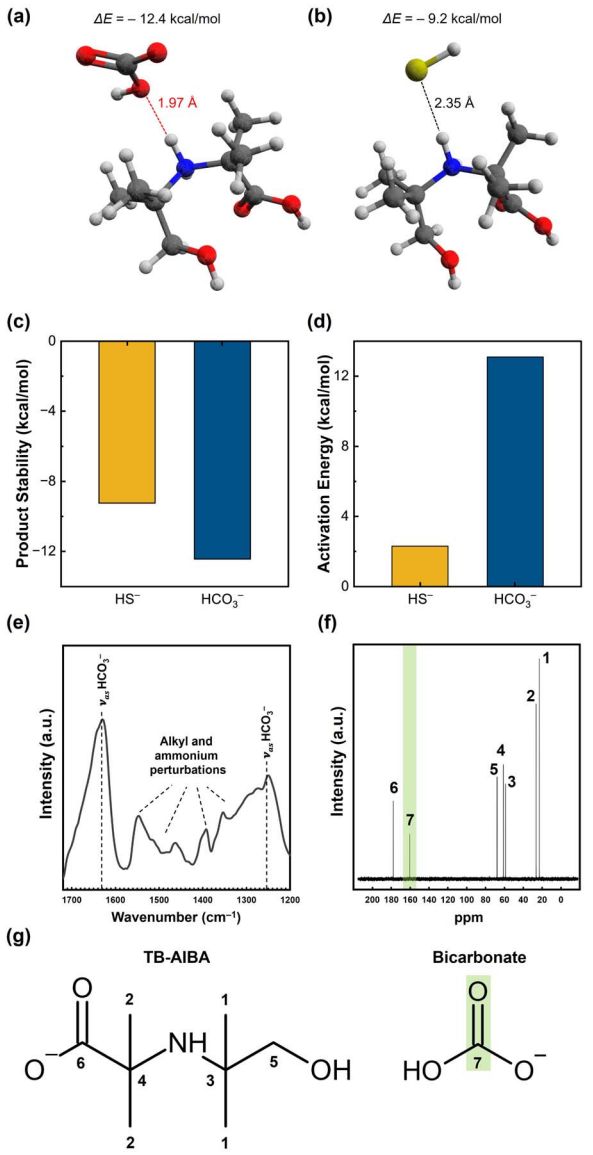

Fig. 4 Molecular configurations of (a) bicarbonate reaction products and (b) hydrosulfide reaction products for carrier TB-AIBA. Color code: carbon (grey), nitrogen (blue), oxygen (red), and hydrogen (white). Red dashed lines represent a hydrogen bond; black dashed lines represent the main atomic distance. DFT-computed (c) product stabilities, and (d) activation energy barriers for the reactions of TB-AIBA with H_2S and CO_2. (e) FTIR spectrum obtained upon *in situ* exposure of PVA/TB-AIBA FTM to 20% CO_2 in N_2 at 110 °C. (f) ^{13}C NMR spectrum obtained upon exposing a 0.5 M solution of TB-AIBA to CO_2 at ambient temperature. The CO_2 loading is controlled to 0.2 M. (g) Chemical structures of TB-AIBA and the bicarbonate anion. The numbering of the carbon atoms corresponds to the peak labels in subfigure (f).

This indicates strong competition between H_2S and CO_2 for the amine carriers, negatively affecting both H_2S and CO_2 facilitation within the FTM. Conversely, for the TB-AIBA-based FTM, the H_2S permeance is strongly dependent on the feed composition. As the H_2S concentration is varied between 0.5–30%, the H_2S permeance shows an initial steep drop, followed by a slower, more gradual decrease, a trend characteristic of carrier saturation. In comparison, the CO_2 permeance does not vary appreciably and remains constant at *ca.* 30 GPU (see Table S4†). This suggests very weak reactive transport of CO_2, implying that CO_2 permeation occurs primarily through solution-diffusion.

An equation was derived for describing H_2S permeance (P_{H_2S}) under conditions of competitive facilitated transport[34,37,72] (see Section S5† for the derivation):

$$P_{H_2S} = \frac{1}{\sqrt{\gamma_{H_2S} x_{H_2S} + \gamma_{CO_2} x_{CO_2}}} \quad (1)$$

Open Access Article. Published on 27 September 2024. Downloaded on 4/2/2026 8:34:18 PM.
This article is licensed under a Creative Commons Attribution-NonCommercial 3.0 Unported Licence.

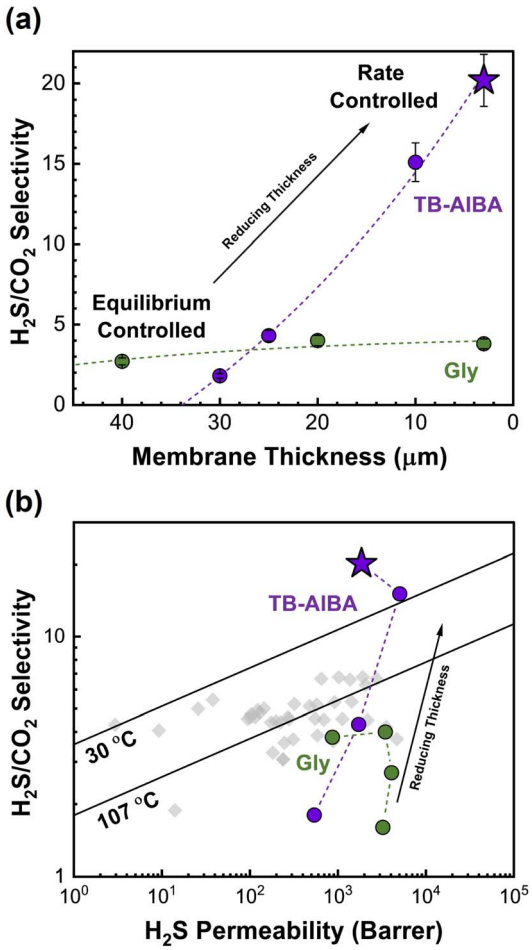

Fig. 5 Mixed-gas H_2S/CO_2 separation performance of FTMs tested at 107 °C and 7 bar feed pressure using a feed composition of 1.0% H_2S in balance CO_2 (dry basis, see Section S1.5† for more details). (a) Effect of FTM thickness on the H_2S/CO_2 selectivity of TB-AIBA-based and Gly-based FTMs. (b) H_2S/CO_2 separation performances of TB-AIBA and Gly-based FTMs against the H_2S/CO_2 upper bounds. The grey markers represent literature data.[38–40,65–69] The black lines represent the H_2S/CO_2 upper bounds, calculated as per Rowe *et al.*[70] Note that the drop in H_2S permeability for the thinnest FTMs is attributed to the significant interfacial reaction resistance, and does not correspond to a drop in H_2S permeance (see Section S4† for more details). The dashed lines are provided to guide the reader's eyes.

wherein γ_{H_2S} and γ_{CO_2} describe the carrier's affinity to H_2S and CO_2, respectively. x_{H_2S} and x_{CO_2} represent the feed mole fractions of H_2S and CO_2, respectively. The values of γ_{H_2S} and γ_{CO_2}, presented in Table 1, were obtained by fitting eqn (1) to the carrier saturation curves in Fig. 6. Comparing the γ_{H_2S} values for the Gly- and TB-AIBA-based FTMs, it is interesting to note that both FTMs possess similar H_2S affinity, confirming that the reaction is insensitive to amine structure. However, the TB-AIBA FTM has much lower CO_2 affinity, freeing up more carriers to facilitate H_2S transport. The fitting suggests that H_2S facilitation is over 40 times higher than CO_2 facilitation within the TB-AIBA FTM (for comparison, the same ratio is *ca.* 4 in the Gly-based FTM). TB-AIBA is nearly inert to CO_2 and facilitates H_2S exclusively, leading to the distinctive carrier saturation curve.

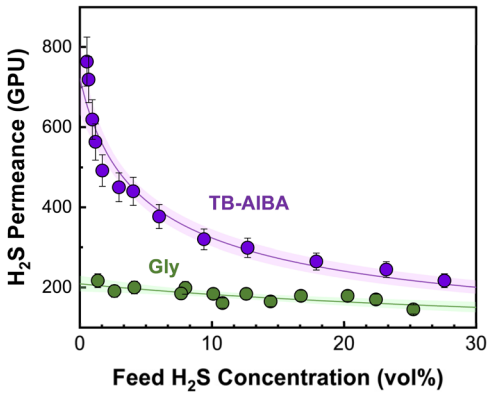

Fig. 6 Effect of feed H_2S concentration on H_2S permeances of TB-AIBA and Gly-based FTMs (GPU: Gas Permeation Unit. 1 GPU = 10^{-6} cm^3(STP) cm^{-2} s^{-1} $cmHg^{-1}$). 3 μm-thick FTMs were tested at 107 °C and 7 bar feed pressure, at feed H_2S concentrations of 0.5–30%, with the balance gas being CO_2 (dry basis). The solid lines represent the best fits by eqn (1).

Table 1 Fitting parameters based on eqn (1) for Gly and TB-AIBA FTMs

Membrane	γ_{H_2S} (10^{-5} GPU^{-2})	γ_{CO_2} (10^{-5} GPU^{-2})
TB-AIBA FTM	7.84 ± 0.66	0.19 ± 0.02
Gly FTM	9.43 ± 1.50	2.29 ± 0.19

Conclusions

In summary, kinetically-controlled separation has been achieved by an exceptionally sterically hindered amine FTM, enabling an unprecedented H_2S/CO_2 selectivity of *ca.* 20. For the competing hydrosulfide and bicarbonate formation reactions, decreasing membrane thickness enhances the facilitation of the kinetic product, *i.e.*, H_2S. Thus, the 3 μm-thick TB-AIBA FTM shows minimal CO_2 facilitation and exhibits remarkable H_2S/CO_2 selectivity. These findings further our understanding of competitive reactive transport in FTMs and address a knowledge gap which hinders their practical applications.

Data availability

The authors confirm that data supporting the findings of this article are available within the article and the ESI.†

Author contributions

S. Rao: conceptualization, methodology, investigation, writing – original draft. X. Deng, C. Zhou, and B. Prasad: investigation and discussion. Y. Han: conceptualization, discussion, writing – reviewing & editing. L.-C. Lin: discussion, writing – reviewing & editing. W.S. Winston Ho: conceptualization, supervision, writing – review & editing.

Conflicts of interest

There are no conflicts to declare.

This journal is © The Royal Society of Chemistry 2024

Open Access Article. Published on 27 September 2024. Downloaded on 4/2/2026 8:34:18 PM. This article is licensed under a Creative Commons Attribution-NonCommercial 3.0 Unported Licence.

Acknowledgements

We thank Dr Ting-Yu Chen, Dr Ruizhi Pang, and Dr Yehiya Khalifa at The Ohio State University for their assistance and guidance in conducting the NMR, SEM and XPS measurements included in this work. We would also like to thank Katharina Daniels, José D. Figueroa, and David Lang of the U.S. Department of Energy – National Energy Technology Laboratory (DOE-NETL) for their helpful discussions. We gratefully acknowledge the funding from DOE-NETL under grant DE-FE0031635 and the Ohio Department of Development under grant OER-CDO-D-19-13. This work was supported in part by the Department of Energy under Award Number DE-FE0031635 with substantial involvement from the National Energy Technology Laboratory, Pittsburgh, PA, USA.

References

1 A. Fayazi, M. Arabloo and A. H. Mohammadi, *J. Nat. Gas Sci. Eng.*, 2014, **16**, 8–17.
2 K. Ramasubramanian, Y. Zhao and W. S. W. Ho, *AIChE J.*, 2013, **59**, 1033–1045.
3 C. N. Okonkwo, H. Fang, D. S. Sholl, J. E. Leisen and C. W. Jones, *ACS Sustainable Chem. Eng.*, 2020, **8**, 10102–10114.
4 B. Doujaiji and J. A. Al-Tawfiq, *Ann. Saudi Med.*, 2010, **30**, 76–80.
5 M. Yadav, M. H. Sliem, A. M. Abdullah, K. M. Youssef and N. H. Al-Qahtani, *Sustainability*, 2022, **14**, 8015.
6 E. F. Diaz, J. G. Gonzalez-Rodriguez, A. Martinez-Villafañe and C. Gaona-Tiburcio, *J. Appl. Electrochem.*, 2010, **40**, 1633–1640.
7 R. W. Baker, *Ind. Eng. Chem. Res.*, 2002, **41**, 1393–1411.
8 S. Dara, A. A. AlHammadi, A. S. Berrouk, F. Al Khasawneh, A. Al Shaiba and Y. F. AlWahedi, *J. Cleaner Prod.*, 2018, **201**, 974–987.
9 A. Al-Amri and U. Zahid, *Energy Fuels*, 2020, **34**, 2545–2552.
10 J.-G. Wagenfeld, K. Al-Ali, S. Almheiri, A. F. Slavens and N. Calvet, *Waste Manage.*, 2019, **95**, 78–89.
11 J. Liu, Y. Wei, P. Li, Y. Zhao and R. Zou, *J. Phys. Chem. C*, 2017, **121**, 13249–13255.
12 Y. Huang and R. Wang, *J. Mater. Chem. A*, 2019, **7**, 12105–12114.
13 C. N. Okonkwo, J. J. Lee, A. De Vylder, Y. Chiang, J. W. Thybaut and C. W. Jones, *Chem. Eng. J.*, 2020, **379**, 122349.
14 C. N. Okonkwo, C. Okolie, A. Sujan, G. Zhu and C. W. Jones, *Energy Fuels*, 2018, **32**, 6926–6933.
15 S. Rao, Y. Han and W. S. W. Ho, *J. Membr. Sci.*, 2023, **686**, 121989.
16 A. K. Chakraborty, G. Astarita and K. B. Bischoff, *Chem. Eng. Sci.*, 1986, **41**, 997–1003.
17 P. V. Danckwerts, *Chem. Eng. Sci.*, 1979, **34**, 443–446.
18 G. Sartori, W. S. W. Ho, D. W. Savage, G. R. Chludzinski and S. Wlechert, *Sep. Purif. Methods*, 1987, **16**, 171–200.
19 A. K. Saha, S. S. Bandyopadhyay, P. Saju and A. K. Biswas, *Ind. Eng. Chem. Res.*, 1993, **32**, 3051–3055.
20 B. P. Mandal, A. K. Biswas and S. S. Bandyopadhyay, *Sep. Purif. Technol.*, 2004, **35**, 191–202.
21 J.-G. Lu, Y.-F. Zheng and D.-L. He, *Sep. Purif. Technol.*, 2006, **52**, 209–217.
22 W. Y. Lee, S. Y. Park, K. B. Lee and S. C. Nam, *Energy Fuels*, 2020, **34**, 1992–2000.
23 R. W. Baker and K. Lokhandwala, *Ind. Eng. Chem. Res.*, 2008, **47**, 2109–2121.
24 Y. Han and W. S. W. Ho, *J. Membr. Sci.*, 2021, **628**, 119244.
25 A. Hussain and M.-B. Hägg, *J. Membr. Sci.*, 2010, **359**, 140–148.
26 I. Taniguchi, S. Duan, T. Kai, S. Kazama and H. Jinnai, *J. Mater. Chem. A*, 2013, **1**, 14514.
27 I. Taniguchi, T. Kai, S. Duan, S. Kazama and H. Jinnai, *J. Membr. Sci.*, 2015, **475**, 175–183.
28 S. Rafiq, L. Deng and M.-B. Hägg, *ChemBioEng Rev.*, 2016, **3**, 68–85.
29 S. Park, O. Morales-Collazo, B. Freeman and J. F. Brennecke, *Angew. Chem., Int. Ed.*, 2022, **61**, e202202895.
30 T.-Y. Chen, X. Deng, L.-C. Lin and W. S. W. Ho, *J. Membr. Sci.*, 2022, **645**, 120195.
31 S. Janakiram, F. Santinelli, R. Costi, A. Lindbråthen, G. M. Nardelli, K. Milkowski, L. Ansaloni and L. Deng, *Chem. Eng. J.*, 2021, **413**, 127405.
32 A. Matsuoka, A. Otani, E. Kamio and H. Matsuyama, *Sep. Purif. Technol.*, 2022, **280**, 119847.
33 J. D. Way and R. D. Noble, *J. Membr. Sci.*, 1989, **46**, 309–324.
34 A. Dindi, R. D. Noble and C. A. Koval, *J. Membr. Sci.*, 1992, **65**, 39–45.
35 S. L. Matson, C. S. Herrick and W. J. Ward, *Ind. Eng. Chem. Process Des. Dev.*, 1977, **16**, 370–374.
36 R. Quinn, J. B. Appleby and G. P. Pez, *Sep. Sci. Technol.*, 2002, **37**, 627–638.
37 S. Li, Z. Wang, W. He, C. Zhang, H. Wu, J. Wang and S. Wang, *Ind. Eng. Chem. Res.*, 2014, **53**, 7758–7767.
38 C. A. Scholes, S. E. Kentish and G. W. Stevens, *Sep. Purif. Rev.*, 2009, **38**, 1–44.
39 D. J. Harrigan, J. Yang, B. J. Sundell, J. A. Lawrence, J. T. O'Brien and M. L. Ostraat, *J. Membr. Sci.*, 2020, **595**, 117497.
40 D. J. Harrigan, J. A. Lawrence, H. W. Reid, J. B. Rivers, J. T. O'Brien, S. A. Sharber and B. J. Sundell, *J. Membr. Sci.*, 2020, **602**, 117947.
41 M. Narimani, S. Amjad-Iranagh and H. Modarress, *J. Mol. Liq.*, 2017, **233**, 173–183.
42 H. M. Stowe, L. Vilčiauskas, E. Paek and G. S. Hwang, *Phys. Chem. Chem. Phys.*, 2015, **17**, 29184–29192.
43 S. Gangarapu, A. T. M. Marcelis, Y. A. Alhamed and H. Zuilhof, *ChemPhysChem*, 2015, **16**, 3000–3006.
44 X. Deng, C. Zou, Y. Han, L.-C. Lin and W. S. W. Ho, *J. Phys. Chem. C*, 2020, **124**, 25322–25330.
45 H. M. Stowe and G. S. Hwang, *Phys. Chem. Chem. Phys.*, 2017, **19**, 32116–32124.
46 T. Davran-Candan, *J. Phys. Chem. A*, 2014, **118**, 4582–4590.
47 W.-C. Yu and G. Astarita, *Chem. Eng. Sci.*, 1987, **42**, 419–424.

Open Access Article. Published on 27 September 2024. Downloaded on 4/2/2026 8:34:18 PM.
This article is licensed under a Creative Commons Attribution-NonCommercial 3.0 Unported Licence.

48 L. Ansaloni, Y. Zhao, B. T. Jung, K. Ramasubramanian, M. G. Baschetti and W. S. W. Ho, *J. Membr. Sci.*, 2015, **490**, 18–28.
49 S. D. Rychnovsky, T. Beauchamp, R. Vaidyanathan and T. Kwan, *J. Org. Chem.*, 1998, **63**, 6363–6374.
50 K. Zhang, B. B. Noble, A. C. Mater, M. J. Monteiro, M. L. Coote and Z. Jia, *Phys. Chem. Chem. Phys.*, 2018, **20**, 2606–2614.
51 Z. Dai, J. Deng, L. Ansaloni, S. Janakiram and L. Deng, *J. Membr. Sci.*, 2019, **578**, 61–68.
52 J. Zou and W. S. W. Ho, *J. Membr. Sci.*, 2006, **286**, 310–321.
53 Y. Chen, L. Zhao, B. Wang, P. Dutta and W. S. W. Ho, *J. Membr. Sci.*, 2016, **497**, 21–28.
54 Z. Zhang, S. Rao, Y. Han, R. Pang and W. S. W. Ho, *J. Membr. Sci.*, 2021, **638**, 119696.
55 T.-Y. Chen, X. Deng, L.-C. Lin and W. S. W. Ho, *J. Membr. Sci.*, 2023, **671**, 121309.
56 X. Deng, Y. Han, L.-C. Lin and W. S. W. Ho, *Sep. Purif. Technol.*, 2022, **299**, 121601.
57 W. C. Wilfong, C. S. Srikanth and S. S. C. Chuang, *ACS Appl. Mater. Interfaces*, 2014, **6**, 13617–13626.
58 D. D. Miller and S. S. C. Chuang, *J. Phys. Chem. C*, 2016, **120**, 25489–25504.
59 G. S. Foo, J. J. Lee, C. Chen, S. E. Hayes, C. Sievers and C. W. Jones, *ChemSusChem*, 2017, **10**, 266–276.
60 D. Wu, C. Sun, P. K. Dutta and W. S. W. Ho, *J. Membr. Sci.*, 2017, **534**, 33–45.
61 J. J. Lee, C.-J. Yoo, C.-H. Chen, S. E. Hayes, C. Sievers and C. W. Jones, *Langmuir*, 2018, **34**, 12279–12292.
62 S. G. Pate, H. Xu and C. P. O'Brien, *J. Mater. Chem. A*, 2022, **10**, 4418–4427.
63 O. Vopička, V. Hynek and V. Rabová, *J. Membr. Sci.*, 2010, **350**, 217–225.
64 J. H. Meldon and A. Dutta, *Chem. Eng. Sci.*, 1994, **49**, 689–697.
65 Y. Ma, H. Guo, R. Selyanchyn, B. Wang, L. Deng, Z. Dai and X. Jiang, *J. Mater. Chem. A*, 2021, **9**, 20211–20240.
66 S. Rao, B. Prasad, Y. Han and W. S. W. Ho, *Energies*, 2023, **16**, 5713.
67 G. Chatterjee, A. A. Houde and S. A. Stern, *J. Membr. Sci.*, 1997, **135**, 99–106.
68 A. Hayek, Y. A. Shalabi and A. Alsamah, *Sep. Purif. Technol.*, 2021, **277**, 119535.
69 C. J. Orme and F. F. Stewart, *J. Membr. Sci.*, 2005, **253**, 243–249.
70 B. W. Rowe, L. M. Robeson, B. D. Freeman and D. R. Paul, *J. Membr. Sci.*, 2010, **360**, 58–69.
71 Y. Zhao, B. T. Jung, L. Ansaloni and W. S. W. Ho, *J. Membr. Sci.*, 2014, **459**, 233–243.
72 F. Gioia and G. Astarita, *Ind. Eng. Chem. Fundam.*, 1967, **6**, 370–375.

This journal is © The Royal Society of Chemistry 2024